Carbohydrate Research 344 (2009) 1582–1587

Contents lists available at ScienceDirect

Carbohydrate Research

journal homepage: www.elsevier.com/locate/carres

An NMR investigation of putative interresidue H-bonding in methyl α-cellobioside in solution

Wenhui Zhang [a], Hongqiu Zhao [a], Ian Carmichael [b], Anthony S. Serianni [a,*]

[a] Department of Chemistry and Biochemistry, University of Notre Dame, Notre Dame, IN 46556, United States
[b] Radiation Laboratory, University of Notre Dame, Notre Dame, IN 46556, United States

ARTICLE INFO

Article history:
Received 11 May 2009
Received in revised form 2 June 2009
Accepted 3 June 2009
Available online 7 June 2009

Dedicated to Professor Hans Kamerling on the occasion of his 65th birthday

Keywords:
NMR spectroscopy
H-Bonding
Disaccharide
^{13}C-Enrichment

ABSTRACT

Methyl α-cellobioside (methyl β-D-glucopyranosyl-(1→4)-α-D-glucopyranoside) was labeled with ^{13}C at C4′ for use in NMR studies in DMSO-d_6 solvent to attempt the detection of a trans-H-bond *J*-coupling ($^{3h}J_{COH}$) between C4′ and OH3. Analysis of the OH3 signal at 600 MHz revealed only the presence of two homonuclear *J*-couplings: $^{3}J_{H3,OH3}$ and a smaller, longer range J_{HH}. No evidence for $^{3h}J_{C4',OH3}$ was found. The longer range J_{HH} was traced to $^{4}J_{H4,OH3}$ based on 2D ^{1}H–^{1}H COSY data and inspection of the H2 and H4 signal lineshapes. A limited set of DFT calculations was performed on a methyl cellobioside mimic to evaluate the structural dependencies of $^{4}J_{H2,O3H}$ and $^{4}J_{H4,O3H}$ on the H3–C3–O3–H torsion angle. Computed couplings range from about −0.7 to about +1.1 Hz, with maximal values observed when the C–H and O–H bonds are roughly diaxial.

1. Introduction

Conformational analyses of oligosaccharides involve not only determinations of the preferred geometries and time-dependent motions of their constituent glycosidic linkages and pyranosyl and furanosyl rings, but also assessments of the solution behaviors of exocyclic substituents such as hydroxyl, hydroxymethyl (CH_2OH) and *N*-acetyl groups.[1–6] In recent years, considerable effort has been directed towards improving these determinations partly through the development of more quantitative analyses of NMR spin–spin coupling constants (*J*-couplings) involving ^{13}C and ^{1}H, which are abundant in saccharides. For example, homonuclear ^{13}C–^{13}C spin-couplings provide unique and useful constraints not only to assess *O*-glycosidic linkage geometry[7,8] but also to establish aldohexopyranosyl ring conformation (e.g., $^{3}J_{C1,C6}$ and $^{3}J_{C3,C6}$ values in aldohexopyranosyl rings).[9,10] Karplus or Karplus-like relationships (the latter defined as parameterization of *J*-couplings other than ^{3}J in terms of one or more specific molecular torsion angles)[11] have been described in which equations containing two torsion angle variables are solved simultaneously to allow determinations of correlated conformations in saccharides, information not easily obtained by other experimental means.[12]

Establishing the conformational properties of oligosaccharides in solution is important due to the presumed correlation between their 3D structures and biological functions. Equally important, however, is determining why a specific oligosaccharide behaves as it does: what intrinsic structural forces are at work and how do they interact, and what extrinsic factors (e.g., solvation, context) play a role? Can these factors be quantified?

The role of H-bonding in influencing oligosaccharide structural properties is an example of an extrinsic factor whose importance in dictating oligosaccharide conformation/dynamics in solution has received considerable attention[4,13–18] but still remains unclear. Studies of single-crystal X-ray structures suggest that H-bonding between contiguous residues of an oligosaccharide does occur. For example, in β-(1→4)-linked disaccharides such as methyl α-lactoside (**1**),[19] methyl β-lactoside (**2**)[20] and methyl β-cellobioside (**3**)[21] (Scheme 1), interresidue H-bonding is inferred between O3H (donor) and O5′ (acceptor) based on the O3–O5′ internuclear distance observed in the crystal structures. The role of this H-bonding in dictating preferred linkage geometry in aqueous solution is uncertain, given that competition is likely between this intramolecular H-bonding and intermolecular H-bonding involving solvent water. It is difficult to obtain definitive experimental evidence about specific saccharide H-bonding behavior in solution, and more specifically, how strong/persistent this H-bonding might be. Recent work suggests that $^{1}J_{CH}$ values involving alcoholic carbons might be useful in this regard, since their magnitudes are not only influenced by vicinal lone-pair effects[22] but also by the propensity of the OH group to H-bond in either a donor or acceptor role.[23]

* Corresponding author. Tel.: +1 574 631 7807.
E-mail address: aseriann@nd.edu (A.S. Serianni).

0008-6215/$ - see front matter © 2009 Elsevier Ltd. All rights reserved.
doi:10.1016/j.carres.2009.06.007

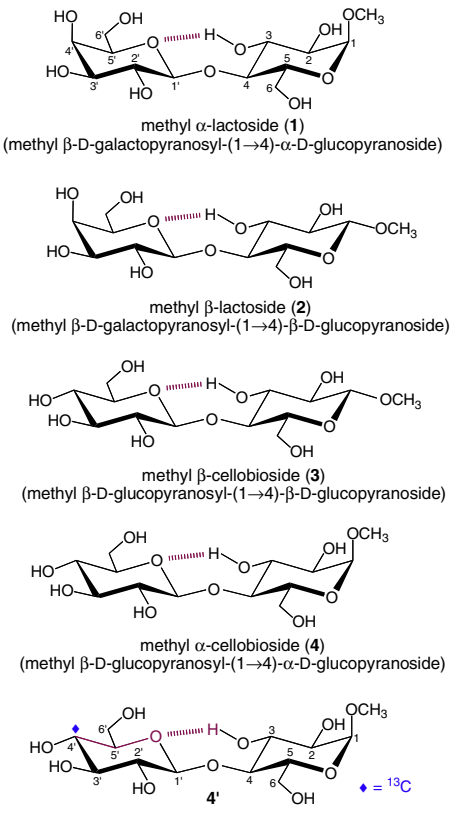

Scheme 1.

The present investigation approaches this general problem from a different vantage point. We reasoned that, if the type of interresidue H-bonding observed in X-ray structures **1**–**3** were present (persistent) in solution, then *J*-coupling across this stable H-bond might be observable, specifically between C4′ and the H-bonded O3H hydrogen (i.e., $^{3h}J_{C4',O3H}$). To investigate this possibility, DFT calculations were initially performed on model structures to estimate the magnitude of this coupling under conditions mimicking full persistence. These calculations yielded predicted $^{3h}J_{C4',O3H}$ values of ~0.1 Hz. The uncertainty in these calculated couplings (~±0.2 Hz) is relatively large, however, so we decided to pursue an experimental investigation of the problem.

2. Results and discussion

Methyl α-cellobioside **4** (Scheme 1), whose solution conformation has been studied previously,[24,25] was chosen as the target disaccharide, selectively labeled with ^{13}C at C4′ (**4′**) (Scheme 1), because (a) synthesis of D-[4-^{13}C]glucose[26] and assembly of the labeled disaccharide are straightforward, and (b) the equatorial C4′–O4′ bond in **4**/**4′** is expected to enhance the $^{3h}J_{C4',O3H}$ value, if it exists, due to the terminal oxygen in-plane effect on $^{3}J_{CH}$ values.[6,27] In addition, in **4**/**4′**, the C4′–C5′–O5′–O3H pseudo-torsion angle approaches 180°, rendering this system ideally suited for detection of a trans-H-bond $^{3}J_{COH}$ if conventional Karplus behavior applies. Synthesis of ^{13}C-labeled disaccharide **4′** is described in Supplementary data.

The 600 MHz ^{13}C{^{1}H} NMR spectrum of **4′** in $^{2}H_2O$ is shown in Figure 1, and ^{13}C spectral parameters are summarized in Table 1. Three intrarresidue J_{CC} values were observed in the labeled β-Glc*p* residue: $^{1}J_{C4',C3'}$ = 39.5 Hz; $^{1}J_{C4',C5'}$ = 41.0 Hz; $^{2}J_{C4',C2'}$ = +2.6 Hz. These couplings are indistinguishable from those reported previously in methyl β-D-glucopyranoside (Table 1).[12] The value of $^{2}J_{C4',C6'}$ was very small or zero, which is consistent with the observed behavior of this coupling in glucopyranosyl rings.[10,12] The dual-pathway $^{3+3}J_{C4',C1'}$ was also very small or zero, consistent with observations in β-Glc*p* rings.[10]

The ^{1}H NMR spectrum of **4′** in $^{2}H_2O$ is shown in Figure 2 and ^{1}H spectral parameters are summarized in Table 2. Several J_{CH} values involving non-exchangeable carbon-bonded protons were measurable: $^{1}J_{C4',H4'}$ = ~147 Hz; $^{2}J_{C4',H3'}$ = ~−5.7 Hz; $^{3}J_{C4',H6'a}$ = ~2.3 Hz; $^{3}J_{C4',H6'b}$ = 1.0 Hz. The vicinal J_{CH} values involving H6′a and H6′b in **4′** are similar to those reported in methyl β-D-glucopyranoside,[12] suggesting similar exocyclic hydroxymethyl conformations, a conclusion supported by the similar $^{3}J_{H5',H6'a/b}$ values. However, differences were observed in $^{1}J_{CH}$ and $^{2}J_{CH}$ values involving C4′ (Table 2),

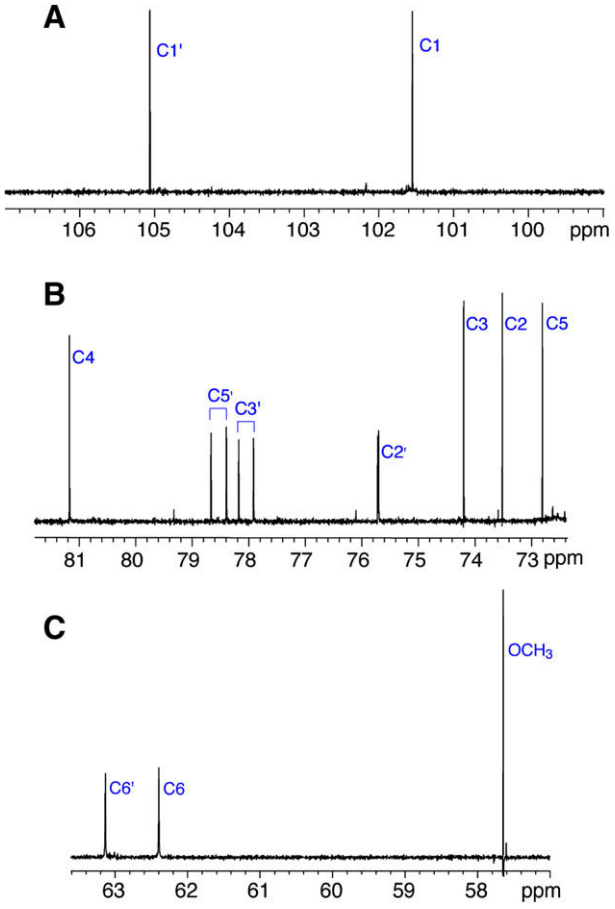

Figure 1. The ^{13}C{^{1}H} NMR spectrum (150 MHz) of **4′** in $^{2}H_2O$ at 22 °C, showing signal assignments and splittings due to ^{13}C–^{13}C spin–spin coupling (Table 1).

Table 1
^{13}C Chemical shifts and ^{13}C–^{13}C spin–spin coupling constants in **4**/**4′**

^{13}C chemical shift (±0.01 ppm)							
Residue	C1/C1′	C2/C2′	C3/C3′	C4/C4′	C5/C5′	C6/C6′	OCH_3
α-Glc	101.55	73.52	74.20	81.17	72.81	62.40	57.65
β-Glc	105.06	75.71	78.05	72.01	78.53	63.13	
^{13}C–^{13}C spin–spin coupling constants (±0.1 Hz)							
Residue	$^{1}J_{C4',C3'}$	$^{1}J_{C4',C5'}$	$^{2}J_{C4',C2'}$				
β-Glc	39.5	41.0	+2.6				
MeβGlc[a]	39.3	41.0	+2.7				

In $^{2}H_2O$; 22 °C; relative to external 3-(trimethylsilyl)-1-propanesulfonic acid sodium salt (DSS).

[a] Couplings in methyl β-D-glucopyranoside were taken from Thibaudeau et al. (Ref. 12).

possibly due to different C–O bond torsional behaviors at C3′ and/or C4′ in the mono- and disaccharide.

Since the aim of the present work was to evaluate the possibility of a trans-H-bond coupling between C4′ and O3H in **4**′, solution conditions were chosen to maximize the likelihood and persistence of this H-bond by studying **4**′ in DMSO-d_6. Under these conditions, competition involving solvent H-bonding was reduced, increasing the likelihood of an O5′···H-O3 interaction.

The partial 600 MHz ^{1}H NMR spectrum of **4**′ in DMSO-d_6 is shown in Figure 3. ^{1}H spectral parameters (non-exchangeable sites) are summarized in Table 3. Assignments of the OH protons were made by analyses of 2D ^{1}H–^{1}H COSY spectra (Figure S1, Supplementary data). A relatively small $^3J_{H3,O3H}$ value (2.1 Hz) (Table 3) was observed, which was interpreted previously in related disaccharides as evidence of a C3–O3 bond torsion consistent with a geometry required for O5′···H–O3 H-bonding.[6,28] This coupling is considerably smaller than other $^3J_{HCOH}$ values in **4** (Table 3), which range from 4.8 to 6.6 Hz. Closer examination of the O3H doublet in **4**′ revealed the presence of a small splitting (0.3 Hz) when moderate resolution enhancement was applied during FID processing (Fig. 3, inset). This splitting was initially assigned to a putative trans-H-bond coupling involving C4′.

To test the above spectral interpretation, the ^{1}H NMR spectrum of **4** in DMSO-d_6 was obtained, with the expectation that the O3H signal in the unlabeled disaccharide would appear as a simple doublet if the additional 0.3 Hz splitting observed in **4**′ was caused by $^{3h}J_{C4',O3H}$. The partial ^{1}H NMR spectrum of **4** is shown in Figure 4, and the ^{1}H–^{1}H couplings measured in this spectrum are summarized in Table 3. The O3H signal observed in **4** is identical to that

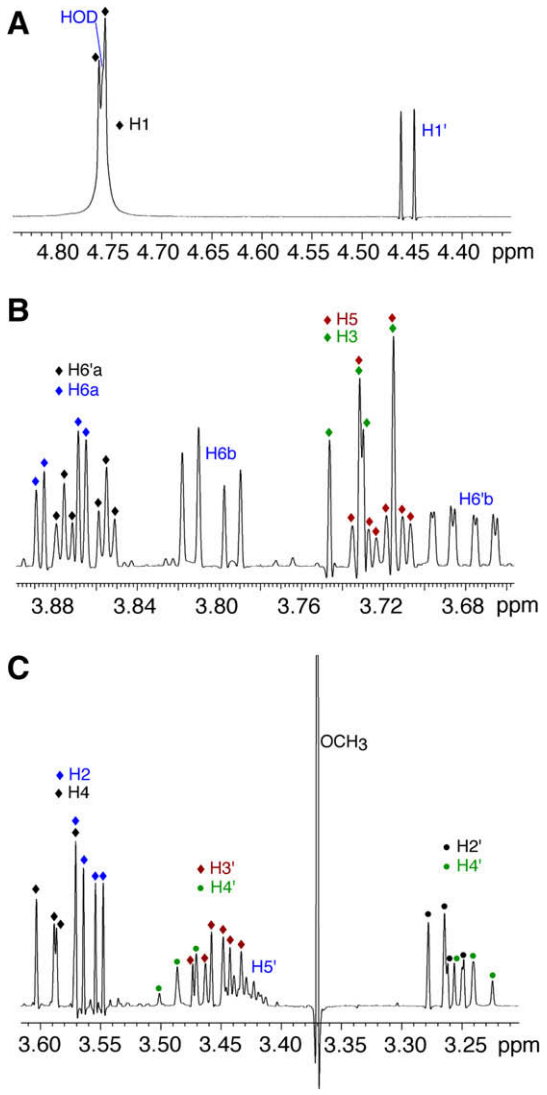

Figure 2. ^{1}H NMR spectrum (600 MHz) of **4**′ in ^2H_2O at 22 °C showing signal assignments (Table 2).

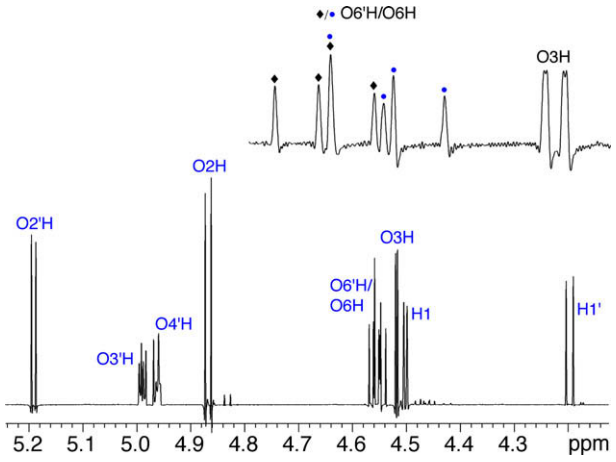

Figure 3. The partial ^{1}H NMR spectrum (600 MHz) of **4**′ in DMSO-d_6 at 22 °C showing signal assignments of the OH and anomeric protons. The inset is an expansion of the O6H/O6′H and O3H signals, showing the additional small splitting of the latter. $^3J_{C4',O3'H}$ = ~2.7 Hz; $^2J_{C4',O4'H}$ = ~ 2 Hz.

Table 2
^{1}H Chemical shifts and ^{1}H–^{1}H and ^{13}C–^{1}H spin–spin coupling constants in **4**/**4**′

^{1}H chemical shift (±0.001 ppm)													
Residue	H1	H2	H3	H4	H5	H6a	H6b	OCH_3					
α-Glc	4.759	3.559	3.731	3.588	3.721	3.877	3.804	3.370					
β-Glc	4.454	3.263	~3.45	3.363	~3.43	3.865	3.681						
^{1}H–^{1}H and ^{13}C–^{1}H spin–spin coupling constants (±0.1 Hz)													
Residue	H1–H2	H2–H3	H3–H4	H4–H5	H5–H6a	H5–H6b	H6a–H6b						
α-Glc	3.8	9.9	8.8	9.9	2.3	4.7	−12.3						
MeαGlc[a]	3.8	9.8	9.2	10.0	2.3	5.6	−12.3						
	H1′–H2′	H2′–H3′	H3′–H4′	H4′–H5′	H5′–H6′a	H5′–H6′b	H6′a–H6′b	C4′–H4′	C4′–H3′	C4′–H5′	C4′–H2′	C4′–H6′a	C4′–H6′b
β-Glc	7.9	9.6	~9.2	~9.8	~2.3	5.9	−12.4	~147	~5.7	nd	~0	~2.3	1.0
MeβGlc[a]	8.0	9.5	9.2	10.0	2.3	6.2	−12.4	144.8	−4.8	−2.9	1.1	2.4	1.2

In ^2H_2O; 22 °C; relative to external 3-(trimethylsilyl)-1-propanesu lfonic acid sodium salt (DSS). H6a and H6′a are defined as the less shielded diastereotopic proton on C6 and C6′, respectively.

[a] Couplings for methyl α- and β-D-glucopyranosides were taken from Thibaudeau et al. (Ref. 12).

Table 3
^{1}H Chemical shifts and ^{1}H–^{1}H spin–spin coupling constants in **4**

^{1}H chemical shift (±0.001 ppm)												
Residue	H1	H2	H3	H4	H5	H6a	H6b	OCH_3				
α-Glc	4.507	3.234	3.491	3.294	3.420	3.674	3.622	3.363				
β-Glc	4.202	2.982	3.144	3.047	3.174	3.685	3.402					
^{1}H–^{1}H spin–spin coupling constants (±0.1 Hz)												
Residue	H1–H2	H2–H3	H3–H4	H4–H5	H5–H6a	H5–H6b	H6a–H6b	H2–O2H	H3–O3H	H6a–O6H	H6b–O6H	
α-Glc	3.6	9.6	8.5	9.9	2.5	4.4	-11.9	6.6	2.1	5.6	6.6	
	H1′–H2′	H2′–H3′	H3′–H4′	H4′–H5′	H5′–H6′a	H5′–H6′b	H6′a–H6′b	H2′–O2′H	H3′–O3′H	H4′–O4′H	H6′a–O6′H	H6′b–O6′H
β-Glc	7.9	9.1	8.8	9.7	2.3	6.5	−11.5	4.9	5.0	5.5	4.8	6.0

In DMSO-d_6; 22 °C; referenced to internal DMSO-d_6 (2.490 ppm). H6a and H6′a are defined as the less shielded diastereotopic proton on C6 and C6′, respectively.

observed in **4′**, that is, it contains 2.1 Hz and 0.3 Hz couplings. These results eliminate the presence of a measurable $^{3h}J_{C4',O3H}$ in **4′**.

The above analyses show that the O3H signal in both **4** and **4′** contains two homonuclear ^{1}H–^{1}H couplings: a 2.1 Hz vicinal $^3J_{H3,O3H}$ and a 0.3 Hz coupling presumably caused by a longer range $^4J_{HH}$ interaction involving either H2 ($^4J_{H2,O3H}$) or H4 ($^4J_{H4,O3H}$).[29] An effort was made to determine whether the H2 or H4 signal in **4**/**4′** contained evidence of a $^4J_{HH}$ interaction. A partial ^{1}H NMR spectrum of **4′** in DMSO-d_6 is shown in Figure 5. The H2 signal contains three couplings, 3.7 Hz, 6.6 Hz, and 9.6 Hz, and these couplings were assigned to $^3J_{H1,H2}$, $^3J_{H2,O2H}$ and $^3J_{H2,H3}$, respectively, based on coupling data in Table 3. The H2 signals were relatively sharp, with no indication of broadening caused by the presence of a small long-range ($^4J_{HH}$) coupling. The H4 signal contains two couplings, 8.5 Hz and 9.9 Hz, and these couplings were assigned to $^3J_{H3,H4}$ and $^3J_{H4,H5}$, respectively, based on coupling data in Table 3. Importantly, the H4 signals, relative to the H2 signals, were broadened, suggestive of the presence of additional long-range ($^4J_{HH}$) coupling(s). The latter could arise from $^4J_{H4,O3H}$, $^4J_{H4,H1'}$ (trans-glycoside)[30] and/or $^4J_{H4,H6a}$/$^4J_{H4,H6b}$. Closer examination of the H4 signals revealed that they contain at least two long-range couplings based on their line shapes. Since the H2 signal shows no evidence of coupling to O3H, the only remaining candidate is H4 whose signal exhibits the expected properties.

A 2D ^{1}H–^{1}H COSY spectrum was obtained on **4** (Fig. 6) to further investigate long-range coupling involving H4. Weak cross peaks correlating H4 with both H1′ and O3H were observed, with the former considerably more intense than the latter. No correlations were detected between H4 and the H6a/H6b sites. These findings indicate that the line broadening observed in the H4 signal (Fig. 5) is attributable to $^4J_{H4,O3H}$ and $^4J_{H4,H1'}$. Since there is no evidence of $^4J_{H2,O3H}$ in the H2 signal in the 1D ^{1}H data (Fig. 5), the small 0.3-Hz splitting of the O3H signal (Figs. 3 and 4) is attributed to $^4J_{H4,O3H}$.

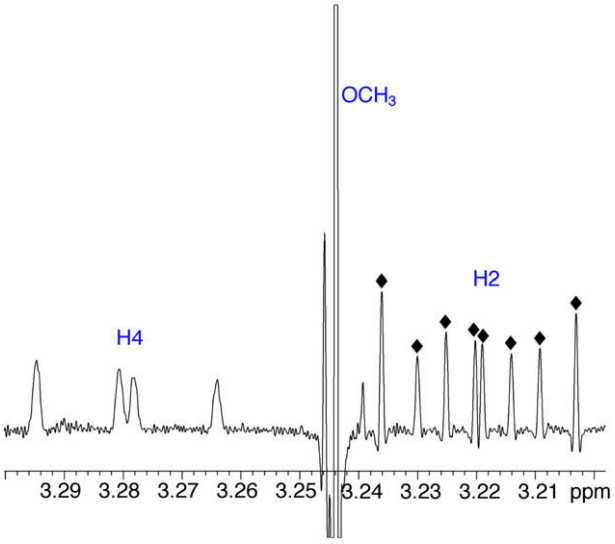

Figure 5. The partial ^{1}H NMR spectrum of **4′** in DMSO-d_6 at 22 °C showing only the H4, OCH_3 and H2 signals. Note the broadened H4 signals, in contrast to the relatively sharp H2 signals.

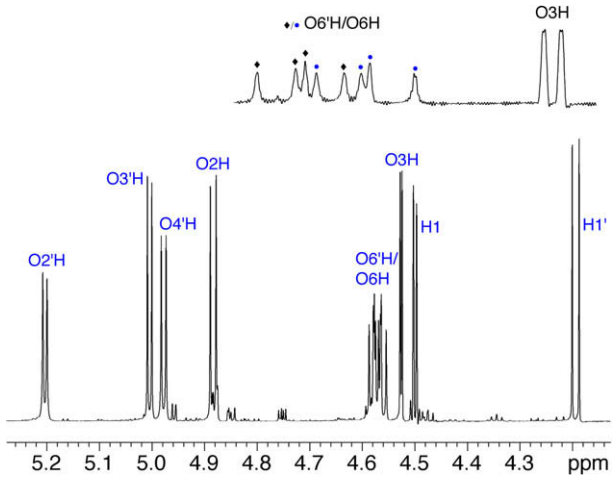

Figure 4. The partial ^{1}H NMR spectrum (600 MHz) of **4** in DMSO-d_6 at 22 °C showing signal assignments of the hydroxyl and anomeric protons. The inset is an expansion of the O6H/O6′H and O3H signals, showing a small splitting in the latter.

The structural dependency of $^4J_{HH}$ involving hydroxyl protons in saccharides was investigated in a limited set of DFT calculations (for computational details, see Supplementary data) performed on **5**, a structural mimic of **4**. In **5**, the H3–C3–O3–H torsion angle was rotated in 15° increments and $^3J_{H3,O3H}$, $^4J_{H2,O3H}$ and $^4J_{H4,O3H}$ values were calculated. In these calculations, the following torsion angles were held fixed: H1′–C1′–O1′–C4 = 31.9° (X-ray value)[21]; C1′–O1′–C4–H4 = -43.7° (X-ray value).[21] Initial values for the C2–C1–O1–CH_3, C1–C2–O2–O2H, and C1′–C2′–O2′–O2′H were set at 165.3°, −175.4° and 165.9°, respectively, and allowed to optimize. In these calculations, it was assumed that anomeric configuration (β in **5**) exerts a minimal effect on the calculated couplings since their pathways are relatively remote from the anomeric center.

The dependence of $^3J_{H3,O3H}$ on the H3–C3–O3–H torsion angle in **5** is shown in Figure 7A. Superimposed on these data is a generalized Karplus dependency for $^3J_{HCOH}$ reported recently by Zhao et al.[6] The close agreement between the two datasets serves as an internal control for the present calculations, and validates the method for use in the $^4J_{HCCOH}$ calculations.

The calculated dependencies of two $^4J_{HCCOH}$, namely $^4J_{H2,O3H}$ and $^4J_{H4,O3H}$, are shown in Figure 7B. In both cases, the calculated couplings range from ∼−0.7 Hz to ∼+1.1 Hz, with maximum coupling observed at H3–C3–O3–O3H torsion angles near 165° and 210° for $^4J_{H2,O3H}$ and $^4J_{H4,O3H}$, respectively. The two curves have similar overall shapes and are phase shifted by ∼45°.

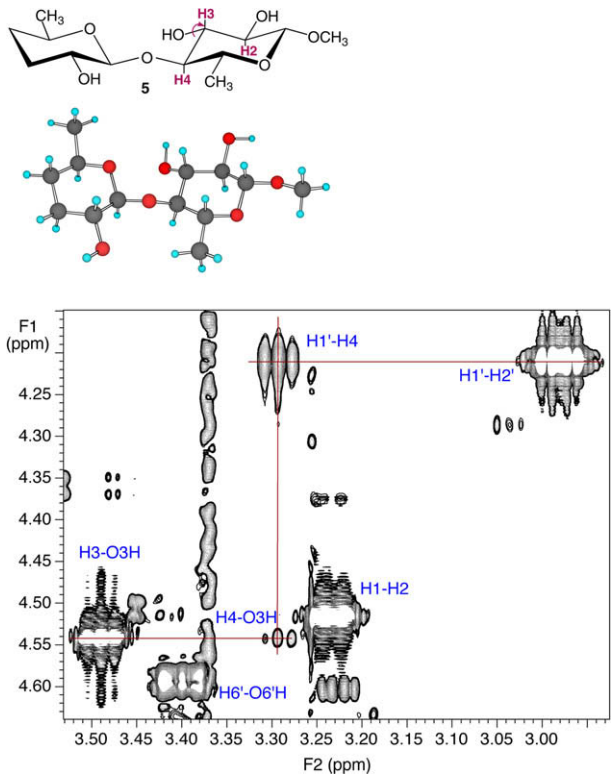

Figure 6. Partial ^{1}H–^{1}H COSY spectrum (600 MHz) of **4** in DMSO-d_6 at 22 °C showing weak cross peaks between H1′–H4 ($^{4}J_{HCOCH}$) and H4–O3H ($^{4}J_{HCCOH}$). The H1–H2, H1′–H2′, H3–O3H and H6′–O6′H cross peaks are also shown.

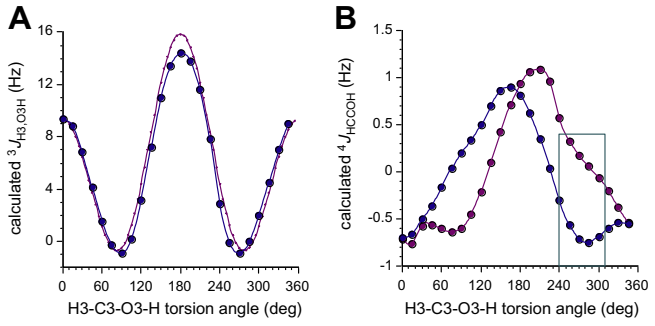

Figure 7. (A) DFT-calculated $^{3}J_{H3,O3H}$ values in **5** as a function of the H3–C3–O3–H torsion angle (blue symbols); red curve is derived from a generalized $^{3}J_{HCOH}$ Karplus equation.[6] (B) DFT-calculated $^{4}J_{H2,O3H}$ (blue symbols) and $^{4}J_{H4,O3H}$ (red symbols) as a function of the H3–C3–O3–H torsion angle in **5**. Area enclosed by the green box approximates the allowed torsion angles for inter-residue O5′…HO3 H-bonding.

Inspection of the data in Figure 7B shows that, in the H3–C3–O3–H torsional regime that allows for inter-residue H-bonding to O5′ (~240–310°), $^{4}J_{H4,O3H}$ is more positive than $^{4}J_{H2,O3H}$. Given that the computed couplings are small, relatively large uncertainties exist in these curves, with absolute values less certain but differences likely to be maintained. Qualitatively, these results are taken to support the experimental observation that the small 0.3-Hz coupling observed at O3H in **4**/**4**′ in DMSO-d_6 is caused by coupling to H4 and not H2. The $^{4}J_{HH}$ calculations support a H3–C3–O3–O3H torsion angle in the 240–310° regime, which is consistent with prior structural interpretations of the 2.1 Hz value of $^{3}J_{H3,O3H}$.[6]

3. Conclusions

This investigation aimed to determine whether a trans-H-bond $^{3}J_{CCOH}$ value could be detected in a β-(1→4)-linked disaccharide in DMSO-d_6 solvent, thus providing direct experimental evidence that this H-bonding is persistent under these solution conditions. Prior evidence of this H-bonding has been indirect, either implied from X-ray crystal structure studies based on observed C3–O3 bond torsions and O3–O5′ internuclear distances, or from solution NMR studies in which aberrant $^{3}J_{H3,O3H}$ values were interpreted as consistent with geometries that allow this H-bonding, and temperature effects on hydroxyl proton chemical shifts were investigated.[6,28]

Despite optimizing the experiment to detect a potential $^{3h}J_{C4',O3H}$ in **4**′, no coupling was detected. Initial observation of a small 0.3-Hz splitting in the O3H signal was traced to long-range $^{4}J_{HH}$ coupling involving H4. The reasons for this failure may lie in (a) the intrinsically very small values of trans-H-bond $^{3h}J_{CCOH}$ couplings, making them inadequate for this type of characterization, or (b) the coupling is detectable but a strong/persistent H-bond in **4** does not exist in DMSO-d_6 solution. The former argument is supported by DFT calculations that predict very small values of $^{3h}J_{CCOH}$, but the negative findings do not allow exclusion of the latter possibility. O'Leary and co-workers[31] have reported analogous $^{2h}J_{HH}$ and $^{3h}J_{HH}$ couplings in conformationally constrained 1,3- and 1,4-diols in DMSO-d_6, with values of <~0.3 Hz.

DFT calculations of long-range $^{4}J_{HH}$ values involving hydroxyl protons are predicted to be as large as +1 Hz, and in some cases may be negative in sign. The two H–C–C–O–H coupling pathways examined in this report are structurally related in that both involve an axial, carbon-bound hydrogen (H2 or H4) coupled to a hydroxyl proton borne by an equatorial hydroxyl group (O3H). This similarity is likely the root cause of the similar C3–O3 bond torsion dependencies; when H3 is approximately anti to O3H, $^{4}J_{H2,O3H}$ and $^{4}J_{H4,O3H}$ are at or near their maximal values. Under these conditions, the coupled hydrogens are in a 1,3-diaxial arrangement, which is known to give measurable $^{4}J_{HH}$ when carbon-bound hydrogens are involved in the coupling (four-bond H–C–C–C–H pathways).[32] In the present work, the structural dependencies of the other two cases were not examined, that is, when the coupled sites are 1,3-diequatorial or 1,3-axial/equatorial. However, these cases, as found for the diaxial case, are expected to mimic the behaviors of analogous H–C–C–C–H, H–C–O–C–H and H–C–C–O–C systems.[30,32,33]

Acknowledgments

This work was supported in part by NIH Grant 59239 (NIGMS) to A.S. and from Omicron Biochemicals, Inc. of South Bend, Indiana. The Notre Dame Radiation Laboratory is supported by Basic Energy Sciences at the Department of Energy; this is document number NDRL 4801.

Supplementary data

Supplementary data associated with this article can be found, in the online version, at doi:10.1016/j.carres.2009.06.007.

References

1. Homans, S. W. *Prog. NMR Spectrosc.* **1990**, *22*, 55–81.
2. Rao, V. S. R.; Qasba, P. K.; Balaji, P. V.; Chandrasekaran, R. *Conformation of Carbohydrates*; Harwood Academic: Chichester, 1998.
3. Serianni, A. S. Carbohydrate Structure, Conformation and Reactivity: NMR Studies with Stable Isotopes. In *Bioorganic Chemistry: Carbohydrates*; Hecht, S., Ed.; Oxford University Press: New York, 1999.
4. Kirschner, K. N; Woods, R. J. *Proc. Natl. Acad. Sci. U.S.A.* **2001**, *98*, 10541–10545.
5. Stenutz, R.; Carmichael, I.; Widmalm, G.; Serianni, A. S. *J. Org. Chem.* **2002**, *67*, 949–958.
6. Zhao, H.; Pan, Q.; Zhang, W.; Carmichael, I.; Serianni, A. S. *J. Org. Chem.* **2007**, *72*, 7071–7082.

7. Bose, B.; Zhao, S.; Stenutz, R.; Cloran, F.; Bondo, P. B.; Bondo, G.; Hertz, B.; Carmichael, I.; Serianni, A. S. *J. Am. Chem. Soc.* **1998**, *120*, 11158–11173.
8. Cloran, F.; Carmichael, I.; Serianni, A. S. *J. Am. Chem. Soc.* **1999**, *121*, 9843–9851.
9. Wu, J.; Bondo, P. B.; Vuorinen, T.; Serianni, A. S. *J. Am. Chem. Soc.* **1992**, *114*, 3499–3505.
10. Bose-Basu, B.; Klepach, T.; Bondo, G.; Bondo, P. B.; Zhang, W.; Carmichael, I.; Serianni, A. S. *J. Org. Chem.* **2007**, *72*, 7511–7522.
11. Klepach, T. E.; Carmichael, I.; Serianni, A. S. *J. Am. Chem. Soc.* **2005**, *127*, 9781–9793.
12. Thibaudeau, C.; Stenutz, R.; Hertz, B.; Klepach, T.; Zhao, S.; Wu, Q.; Carmichael, I.; Serianni, A. S. *J. Am. Chem. Soc.* **2004**, *126*, 15668–15685.
13. Kroon, J.; Kroon-Batenburg, L. M. J.; Leeflang, B. R.; Vliegenthart, J. F. G. *J. Mol. Struct.* **1994**, *322*, 27–31.
14. Hemmingsen, L.; Madsen, D. E.; Esbensen, A. L.; Olsen, L.; Engelsen, S. B. *Carbohydr. Res.* **2004**, *339*, 937–948.
15. Engelsen, S. B.; Monteiro, C.; Hervé du Penhoat, C.; Pérez, S. *Biophys. Chem.* **2001**, *93*, 103–127.
16. Corzana, F.; Motawia, M. S.; Hervé du Penhoat, C.; van den Berg, F.; Blennow, A.; Pérez, S.; Engelsen, S. B. *J. Am. Chem. Soc.* **2004**, *126*, 13144–13155.
17. Almond, A. *Carbohydr. Res.* **2005**, *340*, 907–920.
18. Hansen, P. I.; Larsen, F. H.; Motawia, S. M.; Blennow, A.; Sprual, M.; Dvortsak, P.; Engelsen, S. B. *Biopolymers* **2008**, *89*, 1179–1193.
19. Pan, Q.; Noll, B. C.; Serianni, A. S. *Acta Crystallogr., Sect. C* **2005**, *61*, o674–o677.
20. Stenutz, R.; Shang, M.; Serianni, A. S. *Acta Crystallogr., Sect. C* **1999**, *55*, 1719–1721.
21. Ham, J. T.; Williams, D. G. *Acta Crystallogr., Sect. B* **1970**, *26*, 1373–1383.
22. Serianni, A. S.; Wu, J.; Carmichael, I. *J. Am. Chem. Soc.* **1995**, *117*, 8645–8650.
23. Maiti, N. C.; Zhu, Y.; Carmichael, I.; Serianni, A. S.; Anderson, V. E. *J. Org. Chem.* **2006**, *71*, 2878–2880.
24. Larsson, E. A.; Staaf, M.; Söderman, P.; Höög, C.; Widmalm, G. *J. Phys. Chem. A* **2004**, *108*, 3932–3937.
25. Olsson, U.; Serianni, A. S.; Stenutz, R. *J. Phys. Chem. B* **2008**, *112*, 4447–4453.
26. Serianni, A. S.; Vuorinen, T.; Bondo, P. B. *J. Carbohydr. Chem.* **1990**, *9*, 513–541.
27. Podlasek, C. A.; Wu, J.; Stripe, W. A.; Bondo, P. B.; Serianni, A. S. *J. Am. Chem. Soc.* **1995**, *117*, 8635–8644.
28. Leeflang, B. R.; Vliegenthart, J. F. G.; Kroon-Batenburg, L. M. J.; van Eijck, B. P.; Kroon, J. *Carbohydr. Res.* **1992**, *230*, 41–61.
29. Larsson, E. A.; Ulicny, J.; Laaksonen, A.; Widmalm, G. *Org. Lett.* **2002**, *4*, 1831–1834.
30. Otter, A.; Bundle, D. R. *J. Magn. Reson.* **1995**, *B109*, 194–201.
31. Fierman, M.; Nelson, A.; Khan, S. I.; Barfield, M.; O'Leary, D. J. *Org. Lett.* **2000**, *2*, 2077–2080.
32. Barfield, M.; Dean, A. M.; Fallick, C. J.; Spear, R. J.; Sternwell, S.; Westerman, P. W. *J. Am. Chem. Soc.* **1975**, *97*, 1482–1492.
33. Pan, Q.; Klepach, T.; Carmichael, I.; Reed, M.; Serianni, A. S. *J. Org. Chem.* **2005**, *70*, 7542–7549.